Anti-Inflammatory Effect of Palmatine Chloride on Lipopolysaccharide-Stimulated RAW 264.7 Mouse Macrophages via Calcium-CHOP Pathway

Young-Jin Kim and Wansu Park *

Posted Date: 13 May 2026

doi: 10.20944/preprints202605.0888.v1

Keywords: palmatine chloride; lipopolysaccharide; macrophage; CHOP; cytokine; p38 MAPK; endoplasmic reticulum; nitric oxide; cytosolic calcium

 doi:10.20944/preprints202605.0888.v1

Article

Anti-Inflammatory Effect of Palmatine Chloride on Lipopolysaccharide-Stimulated RAW 264.7 Mouse Macrophages via Calcium-CHOP Pathway

Young-Jin Kim and Wansu Park *

Department of Pathology, College of Korean Medicine, Gachon University, Seongnam 13120, Korea

* Correspondence: pws98@gachon.ac.kr; Tel.: +82-31-750-8821

Abstract

Palmatine chloride (berbericinine, $C_{21}H_{22}ClNO_4$) is a protoberberine alkaloid found in several plants including Rhizoma Coptidis, Cortex Phellodendri, Rhizoma Corydalis, Guduchi (*Tinospora cordifolia*), and *Tinospora sagittata* roots. Palmatine chloride (PA) is known as an inhibitor of dopamine generation. However, its effect on endoplasmic reticulum (ER) stress-related macrophage activation caused by endotoxin (lipopolysaccharide) is not well known yet. In this study, effects of PA on pyroptotic responses of mouse macrophages (RAW 264.7) activated by endotoxin were investigated using Griess reagent assay for nitric oxide (NO) production, fluo-4 assay for cytosolic calcium release, dihydrorhodamine 123 assay for hydrogen peroxide production, multiple cytokine assay for cytokines production, real-time PCR for inflammatory genes transcriptions, and flow cytometry assay for p38 MAPK activation. Results revealed that PA significantly reduced excessive production levels of NO, hydrogen peroxide, pro-inflammatory cytokines (such as interleukin (IL)-6, CCL3 (MIP-1α), and CSF2 (GM-CSF)), and cytosolic calcium release in endotoxin-stimulated RAW 264.7, but significantly increased the production of anti-inflammatory cytokine IL-10. PA inhibited endotoxin-induced transcripts of *Chop*, *Stat1*, *Fas*, and *c-Fos* in activated RAW 264.7. It also decreased p38 MAPK phosphorylation and level of Fas in RAW 264.7 stimulated by endotoxin. To further interpret these findings, a network pharmacology-informed analysis based on large-scale literature mining was performed, supporting the multi-target regulatory role of PA in ER stress-related pathways. Briefly, PA exerts anti-inflammatory effects on endotoxin-stimulated RAW 264.7 via calcium-CHOP pathway, consequently reducing endotoxin-induced production of pro-inflammatory mediators (NO, cytokines, etc.) and relieving ER stress-related pyroptotic cascade.

Keywords: palmatine chloride; lipopolysaccharide; macrophage; CHOP; cytokine; p38 MAPK; endoplasmic reticulum; nitric oxide; cytosolic calcium

1. Introduction

Infection caused by bacterial invasion to the human body still threatens human health, although many powerful antibiotics have been developed [1,2]. Therefore, research on natural products with fewer side effects for the development of treatments for bacterial infection continues [3,4]. Many studies have shown that natural products exhibit anti-inflammatory effects by controlling macrophage activation triggered by infectious pathogens [5–7]. To treat infectious diseases, direct removal of infectious pathogens is important. Regulating excessive inflammatory responses caused by infection is also meaningful. Lipopolysaccharides (LPS) are endotoxins found in the outer membrane of gram-negative bacteria [8,9]. Because macrophages stimulated by endotoxin release large amounts of cytokines and nitrogen oxides (NO), it is meaningful to perform research on natural products that can regulate LPS-induced production of inflammatory mediators in macrophages.

 doi:10.20944/preprints202605.0888.v1

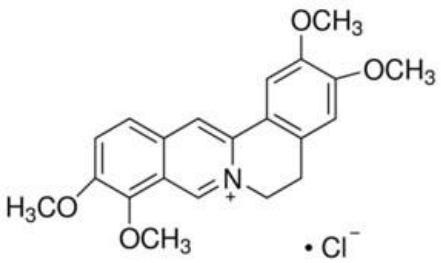

Figure 1. Chemical structure of palmatine chloride (PA).

Macrophage activation is related to many inflammatory diseases. Many studies have been conducted on endoplasmic reticulum (ER) stress and transcription factor C/EBP homologous protein (CHOP) pathway related to macrophage activation caused by various stimuli such as bacterial infection or free cholesterol. Our previous study has shown that baicalin can inhibit inflammatory response of RAW 264.7 mouse macrophages stimulated by LPS through calcium-CHOP pathway involved in ER stress cascade [7]. In other words, ER stress is an important mechanism involved in the activation of macrophages caused by endotoxins. ER stress in macrophages can be caused by free cholesterol-induced unfolded protein responses [10–12]. It can also be caused by infectious pathogens such as endotoxins, leading to apoptosis accompanied by an inflammatory reaction [13,14]. In fact, apoptosis of macrophages due to ER stress proceeds through an increase in cytosolic calcium [15–17]. Thus, natural products that can control the increase of cytosolic calcium in macrophages stimulated by infectious substances should be able to suppress the activation of macrophages and relieve ER stress known to induce inflammatory apoptosis. LPS might activate macrophages to produce various cytokines through p38 mitogen-activated protein kinase (MAPK) signaling [18]. Wang and Ron [19] have reported that the transcription factor CHOP pathway might be activated by p38 MAPK. Endotoxin-induced lung inflammation is exacerbated by an inflammatory response of endotoxin-stimulated macrophages caused by ER stress and CHOP activated by p38 MAPK [20]. Interestingly, Krupkova et al. [21] have reported that p38 MAPK and CHOP can mediate increased expression of interleukin-6 (IL-6) in ER stress-related inflammation in human intervertebral disc.

NO as a free radicals is one of reactive nitrogen species (RNS). In addition to its vasodilatory action, NO can also damage surrounding tissues in the inflammatory process [22–24]. It has been thought that apoptosis caused by excess NO in macrophages or beta cells can be mediated by DNA damage via p53-dependent pathway [22–25]. However, it has been that NO is another inflammatory mediator that can trigger macrophage apoptosis caused by ER stress by inducing CHOP and depleting ER calcium, meaning that NO can increase cytosolic calcium [25]. In other words, NO produced in large quantities in macrophages stimulated by endotoxins can disturb calcium homeostasis, induce unfolded protein response in ER, and worsen ER stress via CHOP pathway, resulting in macrophage apoptosis and inflammatory responses [26–28]. Reactive oxygen species (ROS) is also increased by an unfolded protein response, exacerbating ER stress, causing apoptosis, and leading to neurodegenerative diseases, atherosclerosis, diabetes mellitus, and inflammation in severe cases [29–31]. Tabas et al. [10] have reported that macrophages with intensified ER stress undergo apoptosis by increasing calcium release from ER due to activation of CHOP, followed by CAMKII-induced ROS production, STAT1 activation, and Fas death receptor (Fas) expression. Seimon et al. [32] have reported that LPS could activate Toll-like receptor 4 (TLR4) in ER-stressed macrophages, in which cytosolic calcium plays a key role. Macrophages stimulated by infectious pathogens such as endotoxins go through a lytic programmed cell death process involving inflammatory reactions such as generating and releasing large amounts of cytokines like IL-6, different from general apoptosis [33–35]. Activator protein 1 (AP-1) is known to be activated in response to various cell stimuli including cytokines, oxidative stress, and infections via p38 MAPK signaling, consequently triggering CHOP pathway [36–38]. Interestingly, Klymenko et al. [39] have reported that AP-1-induced CHOP, an important ER stress transcription factor, can increase the

 doi:10.20944/preprints202605.0888.v1

release of calcium from ER store of macrophages stimulated by infectious pathogens, resulting in apoptosis due to ER stress, which can increase the expression of Fas and activate STAT1.

In a previous study, we reported that berberine can modulate macrophage activation [40]. Interestingly, various studies have demonstrated the pharmacological efficacy of palmatine [41–47], a protoberberine alkaloid and a major component of *Coptis chinensis* and *Phellodendron amurense*. The present study aimed to investigate the effects of palmatine chloride (PA) on LPS-induced macrophage activation, with a particular focus on ER stress and calcium signaling. Furthermore, to extend mechanistic insights beyond experimental observations, a network pharmacology-informed approach based on large-scale literature mining was integrated, enabling a more comprehensive characterization of PA as a multi-target regulator of ER stress, particularly via the calcium–CHOP signaling axis.

2. Results

2.1. Cell Viability

Viabilities of THP-1 incubated with PA at concentrations of 10, 25, and 50 μM were 107.82 ± 11.86%, 109.92 ± 10.36%, and 107.49 ± 14.68%, respectively, of the normal group (Nor) treated with media only (Figure 2A). Viabilities of RAW 264.7 incubated with PA at concentrations of 10, 25, and 50 μM were 116.87 ± 22.49%, 137.96 ± 122.38%, and 115.6 ± 21.38%, respectively, of Nor (treated with media only). (Figure 2B). Based on these results, 10, 25, and 50 μM of PA were used in subsequent experiments.

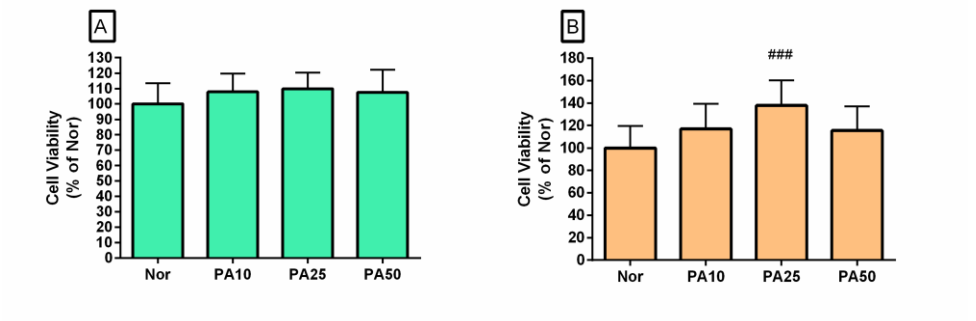

Figure 2. Effects of palmatine chloride on cell viability of THP-1 cells (**A**) and RAW 264.7 cells (**B**). Values are presented as mean ± standard deviation. Nor was the group treated with media alone. PA10 means 10 μM of palmatine chloride, PA25 means 25 μM of palmatine chloride, and PA50 means 50 μM of palmatine chloride. ###, $p < 0.001$ vs. Nor.

2.2. NO Production

Palmatine chloride significantly reduced endotoxins-induced production of NO in activated THP-1 cells (Figure 3A) and RAW 264.7 cells (Figure 3B). In detail, NO production levels in THP-1 cells treated with palmatine chloride at concentrations of 10, 25, and 50 μM were 74.65 ± 8.24%, 73.35 ± 8.69%, and 71.49 ± 8.96%, respectively, of Nor (treated with media only). NO production levels in RAW 264.7 cells treated with palmatine chloride at concentrations of 10, 25, and 50 μM were 66.59 ± 2.17%, 66.54 ± 2.99%, and 61.77 ± 1.91%, respectively, of the control group (Con) treated with LPS (1 μg/mL) alone.

 doi:10.20944/preprints202605.0888.v1

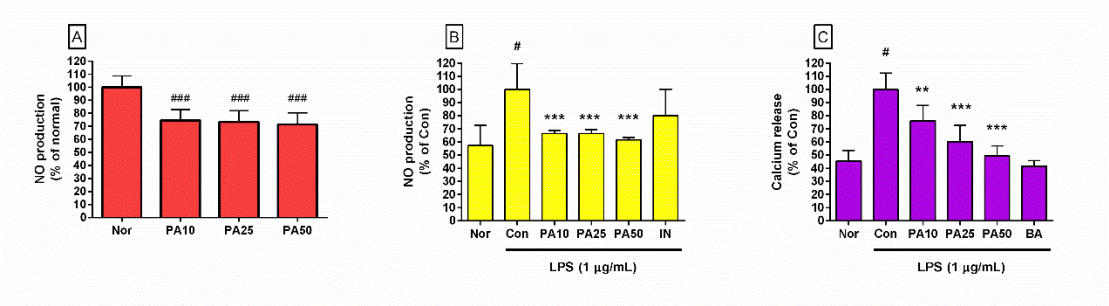

Figure 3. Effects of palmatine chloride on Nitric Oxide (NO) production in THP-1 cells (**A**), NO production in RAW 264.7 cells (**B**), and Calcium release in RAW 264.7 cells (**C**). Values are presented as mean ± standard deviation. Nor was the group treated with media alone; Con, the group treated with lipopolysaccharide (LPS) alone. PA10 means 10 μM of palmatine chloride, PA25 means 25 μM of palmatine chloride, and PA50 means 50 μM of palmatine chloride. IN, indomethacin (0.5 μM); BA, baicalein (25 μM). #, $p < 0.05$ vs. Nor; **, $p < 0.01$ vs. Con; ***, $p < 0.001$ vs. Con.

These results suggest that palmatine chloride can reduce the level of NO overproduced in activated macrophages in a concentration-dependent manner. NO as a free radical is one of RNS. Although NO can act as a vasorelaxant and neurotransmitter, it can cause pathological conditions such as damaging surrounding tissues when it is excessively produced from immune cells such as macrophages during infection-induced excessive inflammatory reactions [22–24]. NO can also cause ER stress in cells such as pancreatic beta cells and macrophages, inducing intracellular calcium release from ER store and promoting CHOP activation with an increase of cytosolic calcium, resulting in cell apoptosis and tissue damage [25–28]. Therefore, the action of palmatine chloride, which inhibits the overproduction of NO in excited macrophages, might modulate ER stress and inflammation related to endotoxin-stimulated macrophages.

2.3. Cytosolic Calcium Release

Palmatine chloride significantly reduced endotoxins-induced release of calcium from ER stores in activated RAW 264.7 (Figure 3C). Cytosolic calcium levels in endotoxins-stimulated RAW 264.7 treated with palmatine chloride at concentrations of 10, 25, and 50 μM were 76.21 ± 11.76%, 60.24 ± 12.46%, and 49.46 ± 7.63% of Con, respectively. These results show that palmatine chloride can decrease cytosolic calcium levels in activated macrophages in a dose-dependent manner. Increasing cytosolic calcium in macrophages excited by stimulating factors such as infectious pathogens is linked to ER stress amplification and induction of the CHOP pathway in activated macrophages, leading to a programmed inflammatory cell lysis due to increased production of inflammatory factors such as cytokines and increased expression of death receptor Fas [10,26–28]. These data suggest that the action of palmatine chloride, which reduces cytosolic calcium in activated macrophages, can alleviate the cascade of apoptosis in macrophages caused by pathogen stimulation by inhibiting ER stress-related calcium pathway.

2.4. Hydrogen Peroxide Production

PA significantly reduced endotoxins-induced production of hydrogen peroxide in RAW 264.7 cells (Figure 4). Production levels of hydrogen peroxide RAW 264.7 treated for 24 h with palmatine chloride at concentrations of 10, 25, and 50 μM were 93.42 ± 6.1%, 83.85 ± 4.62%, and 73.93 ± 6.29% of Con, respectively (Figure 4A). After treatment for 48 h, production levels of hydrogen peroxide in RAW 264.7 cells treated with palmatine chloride at concentrations of 10, 25, and 50 μM were 93.5 ± 6.68%, 85.03 ± 4.99%, and 78.97 ± 7.04% of Con, respectively (Figure 4B). These data indicate that palmatine chloride can inhibit the excessive production of hydrogen peroxide in activated macrophages in a dose-dependent manner. The production of ROS such as hydrogen peroxide can

 doi:10.20944/preprints202605.0888.v1

also be increased by unfolded protein response [29–31]. ROS is known to exacerbate ER stress and cause apoptosis, leading to neurodegenerative diseases, atherosclerosis, diabetes mellitus, and inflammation in severe cases [29–31]. Like RNS, ROS could also destroy infectious microorganisms. However, they can cause toxicity to cells and damage surrounding tissues. Results of this experiment suggest that PA might be able to relieve endotoxins-induced cellular oxidative stress, ER stress, and damage to surrounding tissues by inhibiting excessive production of ROS in pyroptotic macrophages.

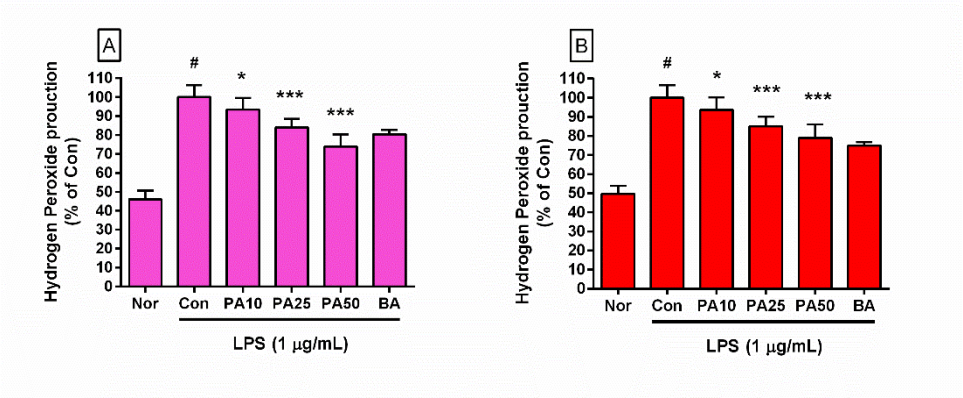

Figure 4. Effects of palmatine chloride on hydrogen peroxide production in RAW 264.7 macrophages after treatment for 24 h (**A**) and 48 h (**B**). Values are presented as mean ± standard deviation. Nor, the group treated with media alone; Con, the group treated with lipopolysaccharide (LPS) alone. PA10 means 10 μM of palmatine chloride, PA25 means 25 μM of palmatine chloride, and PA50 means 50 μM of palmatine chloride. BA, baicalein (25 μM). #, $p < 0.05$ vs. Nor; *, $p < 0.05$ vs. Con; ***, $p < 0.001$ vs. Con.

2.5. Cytokine Production

Palmatine chloride reduced production levels of various cytokines in RAW 264.7 stimulated by endotoxins. Specifically, palmatine chloride at concentrations of 25 and 50 μM significantly decreased production levels of IL-6, granulocyte macrophage colony-stimulating factor (GM-CSF; CSF2), and macrophage inflammatory proteins (MIP)-1α (CCL3). Palmatine chloride at a concentration of 50 μM significantly decreased the production of tumor necrosis factor (TNF)-α, granulocyte colony-stimulating factor (G-CSF; CSF3), MIP-1β (CCL4), and MIP-2 (CXCL2). Additionally, palmatine chloride at concentrations of 10, 25, and 50 μM significantly increased the production of IL-10, a well-known anti-inflammatory cytokine (Figure 5, Table 1). In detail, in endotoxins-stimulated RAW 264.7 treated with palmatine chloride at concentrations of 10, 25, and 50 μM, production levels of IL-6 were 98 ± 2.28%, 97.92 ± 0.52%, and 98.47% ± 0.29% of Con, respectively; those of TNF-α were 91.67 ± 13.71%, 82.6 ± 11.28%, and 83.86 ± 9.35% of Con, respectively; those of GM-CSF were 84.6 ± 18.52%, 59.28 ± 12.08%, and 51.89 ± 11.62% of Con, respectively; those of G-CSF were 99.43 ± 1.87%, 97.61 ± 1.7%, and 96.06 ± 0.14% of Con, respectively; those of MIP-1α were 99.27 ± 1.84%, 96.99 ± 0.82%, and 96.37 ± 0.82% of Con, respectively; those of MIP-1β were 98.7 ± 2.45%, 99.04 ± 1.27%, and 98.19 ± 0.27% of Con, respectively; those of MIP-2 were 100.23 ± 1.23%, 98.99 ± 0.93%, and 98.29 ± 0.19% of Con, respectively; those of LIF were 94.89 ± 9.2%, 84.87 ± 9.73%, and 86.13 ± 9.39% of Con, respectively; and those of IL-10 were 115.5 ± 1.12%, 116.97 ± 3.93%, and 116.54 ± 7.73% of Con, respectively. Contrary to the experimental results of measuring the production of NO and hydrogen peroxide, the decrease in cytokine production by PA10 (10 μM of PA) was not statistically significant. It seems that further research is needed on this.

 doi:10.20944/preprints202605.0888.v1

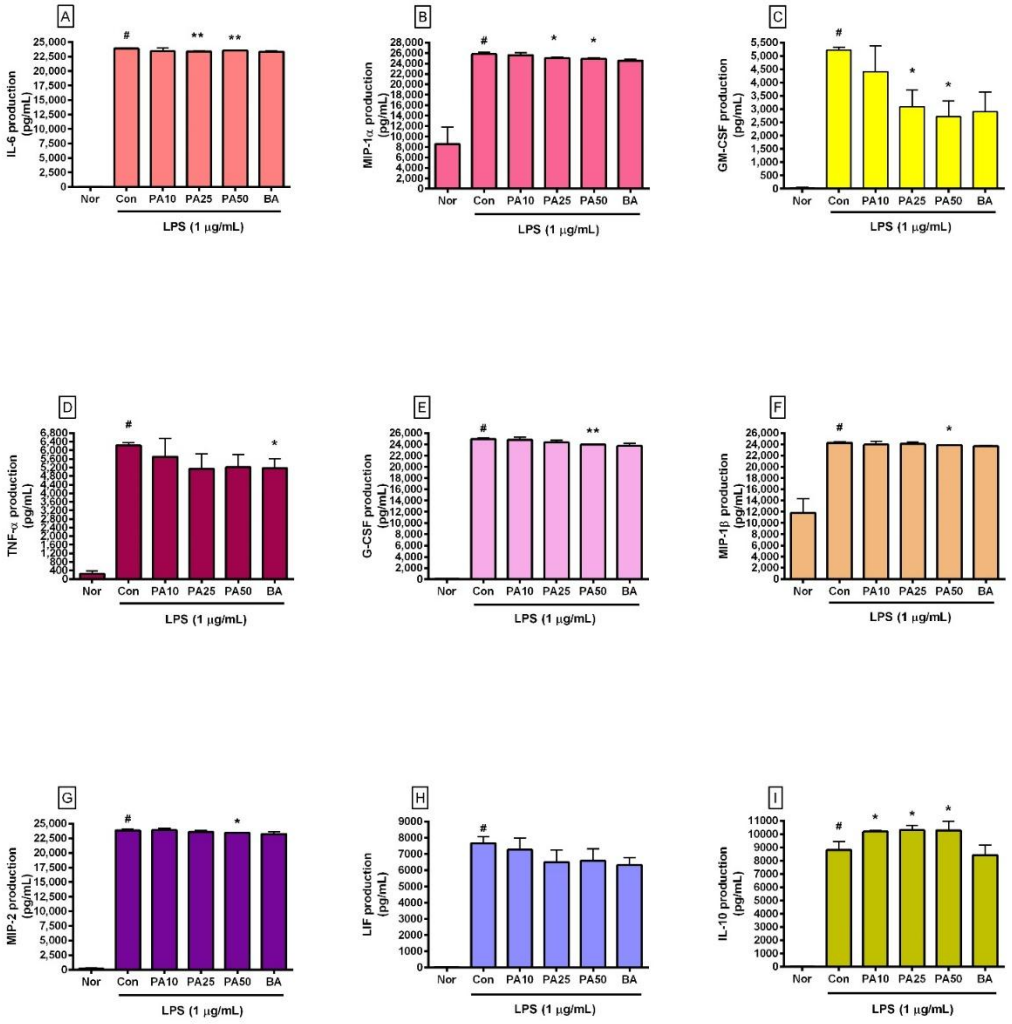

Figure 5. Production of IL-6 (**A**), MIP-1α (**B**), GM-CSF (**C**), TNF-α (**D**), G-CSF (**E**), MIP-1β (**F**), MIP-2 (**G**), LIF (**H**), and IL-10 (**I**) in RAW 264.7 cells. Values are presented as mean ± standard deviation. Nor, the group treated with media alone; Con, the group treated with lipopolysaccharide (LPS) alone. PA10 means 10 μM of palmatine chloride, PA25 means 25 μM of palmatine chloride, and PA50 means 50 μM of palmatine chloride. BA, baicalein (25 μM). #, $p < 0.05$ vs. Nor; *, $p < 0.05$ vs. Con; **, $p < 0.01$ vs. Con; ***, $p < 0.001$ vs. Con.

Table 1. Effects of palmatine chloride on lipopolysaccharide-activated RAW 264.7 cells.

Inflammatory factor	Normal (media only)	Control (LPS alone)	Concentration (μM) of palmatine chloride with lipopolysaccharide (1 μg/mL)		
			10	25	50
IL-6 (pg/mL)	47.00 ± 7.39	23915.00 ± 134.41	23437.50 ± 544.91	23416.50 ± 125.52**	23548.13 ± 68.49**
G-CSF (pg/mL)	79.67 ± 23.16	24929.00 ± 280.38	24787.83 ± 467.42	24332.00 ± 422.63	23947.83 ± 34.40**
IL-10 (pg/mL)	20.19 ± 1.41	8813.88 ± 614.64	10180.00 ± 98.46*	10309.83 ± 346.82*	10271.67 ± 681.40*
MIP-1α (pg/mL)	8570.67 ± 3279.51	25817.33 ± 378.72	25629.17 ± 475.58	25039.67 ± 211.60*	24879.50 ± 210.72*
MIP-2 (pg/mL)	204.17 ± 119.47	23859.63 ± 247.86	23915.67 ± 293.74	23618.67 ± 223.01	23451.50 ± 44.92*
TNF-α (pg/mL)	248.38 ± 126.82	6222.83 ± 136.28	5704.50 ± 852.86	5140.00 ± 701.95	5218.50 ± 581.55*
GM-CSF (pg/mL)	36.25 ± 7.76	5215.00 ± 97.44	4411.67 ± 965.94	3091.33 ± 629.91**	2706.00 ± 606.23**

 doi:10.20944/preprints202605.0888.v1

LIF (pg/mL)	29.00	±	3.91	7657.67	±	422.35	7266.33	±	704.40	6499.00	±	745.09	6595.17	±	719.13
MIP-1β (pg/mL)	11810.17	±	2533.91	24300.25	±	170.14	23984.38	±	596.27	24067.75	±	308.82	23861.00	±	66.05**
Chop mRNA (fold change) changeratio)	1.00	±	0.23	16.39	±	1.53	12.20	±	0.92**	10.86	±	0.93**	7.82	±	0.82***
Fas mRNA (fold change)	1.00	±	0.16	5.41	±	1.61	1.40	±	0.04*	0.75	±	0.12**	0.65	±	0.54**
Stat1 mRNA (fold change)	1.00	±	0.18	1.87	±	0.46	1.06	±	0.06*	1.01	±	0.11*	0.84	±	0.01*
c-Fos mRNA (fold change)	1.00	±	0.34	2.24	±	0.22	1.18	±	0.06**	0.89	±	0.13**	0.88	±	0.40**

Values are presented as mean ± standard deviation (n = 4). *, $p < 0.05$ vs. Con; **, $p < 0.01$ vs. Con; ***, $p < 0.001$ vs. Con.

2.6. Transcriptions of Inflammatory Genes

Palmatine chloride inhibited excessive mRNA expression of *Stat1*, *Chop*, *Fas*, and *c-Fos* in endotoxins-activated RAW 264.7 (Figure 6, Table 1). In LPS-stimulated RAW 264.7 cells treated with PA at concentrations of 10, 25, and 50 μM, transcription levels of *Stat1* were 56.32 ± 3.13%, 53.67 ± 5.61%, and 44.98 ± 0.48% of Con, respectively; those of *Chop* were 74.46 ± 5.62%, 66.28 ± 5.66%, and 47.74 ± 5.02% of Con, respectively; those of *Fas* were 25.93 ± 0.73%, 13.9 ± 2.19%, and 12.03 ± 9.94% of Con, respectively; and those of *c-Fos* were 52.84 ± 2.75%, 39.99 ± 5.66%, and 39.23 ± 17.68% of Con, respectively. Interestingly, c-Fos is a well-known AP-1 transcription factor. AP-1 might be activated in response to various cell stimuli including cytokines, oxidative stress, and infections via p38 MAPK signaling, consequently triggering CHOP pathway [36–38]. Additionally, AP-1-induced CHOP, an important ER stress transcription factor, can increase the release of calcium from ER store of macrophages stimulated by infectious pathogens, resulting in apoptosis due to ER stress, which can increase the expression of Fas and activate STAT1 [39]. Our results suggest that palmatine chloride can relieve ER stress by suppressing the expression of inflammatory genes such as *Chop*, *stat1*, *Fas*, and c-*Fos* in RAW 264.7 cells stimulated by endotoxins via CHOP pathway.

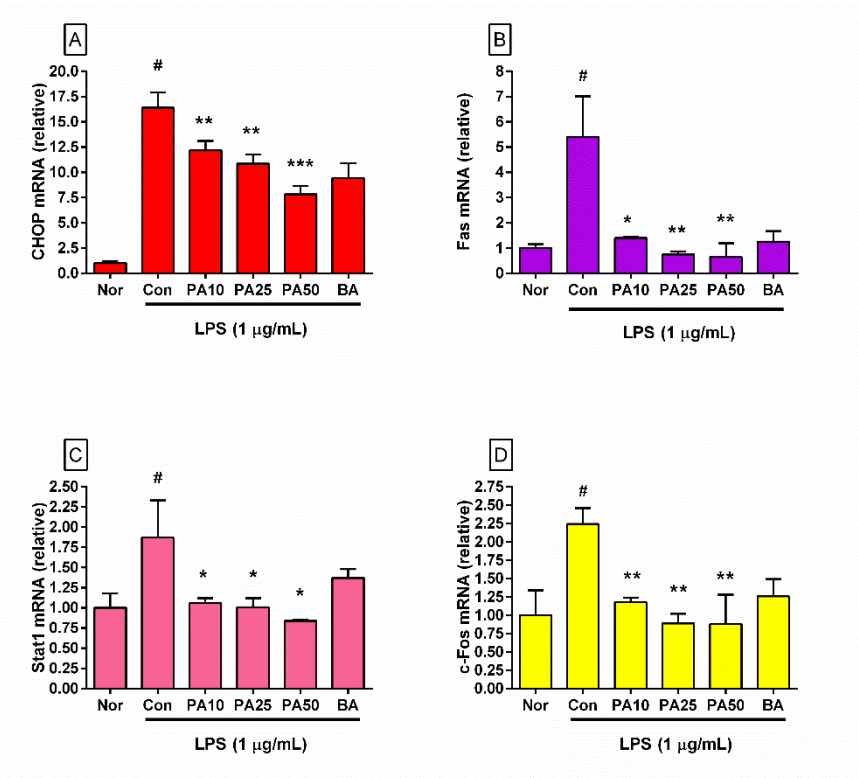

 doi:10.20944/preprints202605.0888.v1

Figure 6. Effects of palmatine chloride on transcription levels of *Chop* (**A**), Fas (**B**), *Stat1* (**C**), and *c-Fos* (**D**) in RAW 264.7 cells. Values are presented as mean ± standard deviation. Nor, the group treated with media alone; Con, the group treated with lipopolysaccharide (LPS) alone. PA10 means 10 μM of palmatine chloride, PA25 means 25 μM of palmatine chloride, and PA50 means 50 μM of palmatine chloride. BA, baicalein (25 μM). #, $p < 0.05$ vs. Nor; *, $p < 0.05$ vs. Con; **, $p < 0.01$ vs. Con; ***, $p < 0.001$ vs. Con.

2.7. Phosphorylation of p38 MAPK and Level of Fas

Phosphorylation levels of p38 MAPK in endotoxins-stimulated RAW 264.7 cells treated with palmatine chloride at concentrations of 10, 25, and 50 μM were 28.4 ± 0.13%, 25.28 ± 4.39%, and 22.77 ± 0.68% of Con, respectively (Figure 7A). Thus, PA could significantly inhibit the activation of p38 MAPK in a dose-dependent manner. Meanwhile, levels of Fas in endotoxins-stimulated RAW 264.7 cells treated with palmatine chloride at concentrations of 10, 25, and 50 μM were 52.88 ± 0.25%, 48.36 ± 1.92%, and 48.55 ± 1.45% of Con, respectively (Figure 7B). These results mean that PA could inhibit the programmed cell death caused by LPS in a concentration-dependent manner.

Macrophages stimulated by endotoxins undergo lytic programmed cell death as ER stress increases and CHOP activation proceeds, including excessive production of inflammatory mediators such as cytokines and NO that occurs through p38 MAPK activation accompanied by increased Fas expression [18–21]. This experimental result indicates that palmatine chloride can inhibit p38 MAPK activation of endotoxins-stimulated macrophages and alleviate ER stress in activated macrophages, thus suppressing the overproduction of pro-inflammatory mediators.

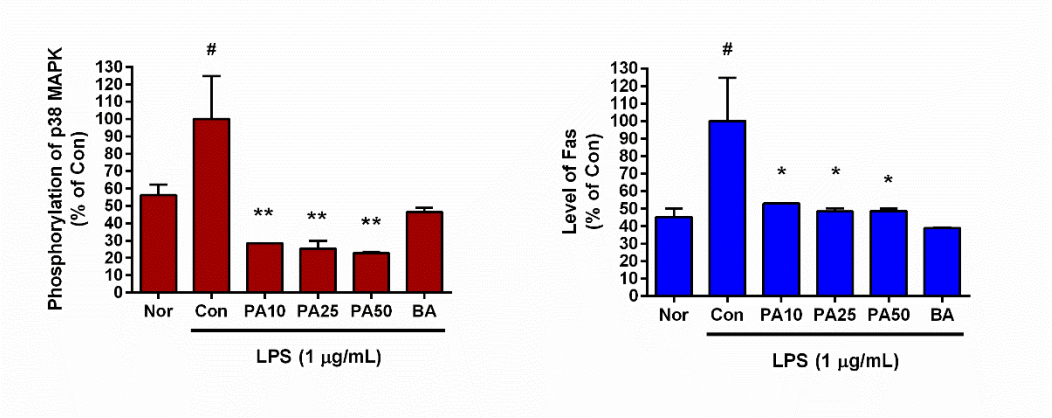

Figure 7. Effects of palmatine chloride on p38 MAPK phosphorylation (**A**) and level of Fas (**B**) in RAW 264.7 cells. Values are presented as mean ± standard deviation. Nor, the group treated with media alone; Con, the group treated with lipopolysaccharide (LPS) alone. PA10 means 10 μM of palmatine chloride, PA25 means 25 μM of palmatine chloride, and PA50 means 50 μM of palmatine chloride. BA, baicalein (25 μM). #, $p < 0.05$ vs. Nor; *, $p < 0.05$ vs. Con; **, $p < 0.01$ vs. Con; ***, $p < 0.001$ vs. Con.

3. Discussion

Although many antibiotics have been developed, bacterial infections are still threatening human health. Therefore, many studies are being conducted on the treatment of bacterial infectious diseases using natural products [3,4]. Additionally, many studies have shown that natural products can relieve excessive inflammation caused by infection by decreasing the production of inflammatory mediators [5–7]. Since various inflammatory mediators are overproduced in the process of macrophage activation caused by infection pathogens, natural products that can suppress the overproduction of inflammatory mediators are thought to be able to regulate macrophage activation caused by infection. In a previous study, our research group reported that berberine can modulate macrophage activation caused by polyinosinic-polycytidylic acid (a double-stranded RNA) and inhibit the excessive production of NO and cytokines [40]. Berberine, a benzylisoquinoline alkaloid, is one of the main components found in *Coptis chinensis* and *Phellodendron amurense*. Interestingly,

 doi:10.20944/preprints202605.0888.v1

palmatine (i.e., a protoberberine alkaloid) with a structure similar to berberine has also been found in *Coptis chinensis* and *Phellodendron amurense*. Traditionally, both *Coptis chinensis* [51] and *Phellodendron amurense* [52] have been used to treat inflammatory diseases. Thus, studies on protoberberine alkaloids such as PA on macrophage activation, an important process for inflammatory pathophysiological phenomena, are meaningful. Interestingly, various studies have reported pharmacological efficacies of palmatine [41–47]. In 2019, Long et al. reported that palmatine had various pharmacological effects such as neuroprotection, anti-bacterial, anti-inflammation, and anti-cancer effects [41]. In 2020, Ekeuku et al. reported the protective effects of palmatine against metabolic syndrome associated with cardiovascular diseases and osteoarthritis due to the antioxidative activities of palmatine [42]. Wang et al. in 2017 reported that palmatine could protect gastric mucosa and inhibit gastric ulcers induced by acetic acid in rats [45]. In 2018, Zhang et al. suggested that palmatine could ameliorate mouse colitis induced by dextran sulfate sodium by regulating gut microbiota and suppressing tryptophan catabolism [46]. Ma et al. in 2016 reported that palmatine could reduce dysplastic change in gut tumorigenesis in ApcMin/+ mice and inflammatory cytokines such as IL-8, CSF2 (GM-CSF), and CSF3 (G-CSF) in gut inflammation [47]. In the current study, results showed that PA treatment at concentrations of 25 and 50 μM for 24 h significantly decreased excessive production of IL-6, CSF2 (GM-CSF), and CCL3 (MIP-1α) in RAW 264.7 cells stimulated by LPS endotoxins. Additionally, PA at a concentration of 50 μM significantly inhibited the excessive production of CSF3 (G-CSF), CXCL2 (MIP-2), CCL4 (MIP-1β), and TNF-α, but significantly increased the production of human cytokine synthesis inhibitory factor (CSIF; IL-10) known to have anti-inflammatory effects. This cytokine production regulation of PA means that PA can modulate macrophage activation caused by stimulation of endotoxins, thereby alleviating excessive inflammatory response in macrophages stimulated by endotoxins.

In a previous study, our research group has shown that baicalin can inhibit the inflammatory response of RAW 264.7 mouse macrophages stimulated by LPS through the calcium-CHOP pathway involved in ER stress cascade [7]. In other words, ER stress is an important mechanism involved in the activation of macrophages caused by endotoxins. ER stress in macrophages can be caused by free cholesterol-induced unfolded protein responses [10–12]. It can also be caused by infectious pathogens such as endotoxins, leading to apoptosis accompanied by an inflammatory reaction [13,14]. In fact, apoptosis of macrophages due to ER stress proceeds through an increase in cytosolic calcium [15–17]. Thus, natural products that can control the increase of cytosolic calcium in macrophages stimulated by pathogenic factors such as endotoxins might be able to suppress the activation of macrophages and relieve ER stress that induces inflammatory apoptosis. In detail, LPS as endotoxins can be released by bacteria when cell walls of Gram-negative bacteria are destroyed or when bacteria die [8,9]. Since macrophages stimulated by pathogens such as endotoxin can release inflammatory mediators such as NO in large quantities, research on natural products that can regulate LPS-induced production of NO in macrophages is meaningful and important. NO as a free radical is one of RNS. It can act as a vasorelaxant and neurotransmitter. It can also cause pathological conditions by damaging surrounding tissues when it is excessively produced from immune cells such as macrophages during an inflammatory response caused by infectious pathogens [22–24]. In fact, apoptosis caused by excess NO in macrophages or beta cells has been thought to be mediated by DNA damage via a p53-dependent pathway [22–25]. However, there have been interesting reports showing that NO is another inflammatory mediator that can trigger macrophage apoptosis caused by ER stress by inducing CHOP and depleting ER calcium, which means that NO can increase cytosolic calcium [25] regardless of the p53-dependent pathway. In other words, NO produced in large quantities in macrophages stimulated by endotoxins can disturb calcium homeostasis and induce an unfolded protein response in ER and worsen ER stress via the CHOP pathway, resulting in macrophage apoptosis and inflammatory responses [26–28]. Tabas et al. [10] have reported that macrophages with intensified ER stress can undergo apoptosis by increasing calcium release from ER due to activation of CHOP, followed by CAMKII-induced ROS production, STAT1 activation, and Fas expression. Of course, macrophages stimulated by infectious pathogens such as endotoxins will

 doi:10.20944/preprints202605.0888.v1

go through apoptosis, a lytic programmed cell death process involving inflammatory reactions such as generating and releasing large amounts of cytokines like IL-6 and TNF-α, which is different from general apoptosis [33–35]. In the present study, PA at concentrations of 10, 25, and 50 μM significantly inhibited NO production and cytosolic calcium release in LPS-stimulated RAW 264.7 as well as excessive transcription of *Chop*, *Fas*, and *Stat1*. These data suggest that PA might modulate macrophage activation induced by endotoxins through ER-stress-related calcium signaling and the CHOP pathway.

The production of ROS is also increased by an unfolded protein response, exacerbating ER stress, causing apoptosis, and leading to neurodegenerative diseases, atherosclerosis, diabetes mellitus, and inflammation in severe cases [29–31]. Our data presented that PA significantly reduced the excessive production of hydrogen peroxide in LPS-induced RAW 264.7. It is well known that ROS can stimulate p38 MAPK signaling [44]. Furthermore, Li et al. [18] have reported that LPS-induced macrophage activation involves massive production of pro-inflammatory cytokines through p38 MAPK signaling. Wang and Ron [19] have reported that the transcription factor CHOP pathway might be activated by p38 MAPK. Endotoxin-induced lung inflammation is exacerbated by the inflammatory response of endotoxin-stimulated macrophages caused by ER stress and CHOP activated by p38 MAPK [20]. Interestingly, Krupkova et al. [21] in 2018 reported that p38 MAPK and CHOP can mediate an increased expression of cytokines such as IL-6 in inflammatory responses caused by ER stress in human intervertebral discs. Our data showed that PA inhibited p38 MAPK activation of RAW 264.7 stimulated by LPS, suggesting that PA could modulate macrophage activation via p38 MAPK signaling accompanied by a decrease in ROS.

ROS and cytokines in LPS-stimulated macrophages are well known to activate AP-1 via p38 MAPK signaling, consequently triggering the CHOP pathway [36–38]. AP-1-induced CHOP can increase the release of calcium from ER store of macrophages stimulated by infectious pathogens, resulting in apoptosis due to ER stress, which can increase the expression of Fas and activate STAT1 [39]. Therefore, PA might be able to relieve ER stress by suppressing the expression of inflammatory genes such as C*hop*, *Fas*, and c-*Fos* in RAW 264.7 cells stimulated by endotoxins via CHOP-related p38 MAPK signaling.

PA has not been widely characterized as a direct regulator of CHOP-mediated endoplasmic reticulum (ER) stress in previous studies. However, accumulating evidence from the palmatine literature indicates that its pharmacological actions converge on multiple upstream and downstream components of the ER stress network, including oxidative stress, calcium homeostasis, MAPK signaling, apoptosis, and autophagy (Figure 8).

 doi:10.20944/preprints202605.0888.v1

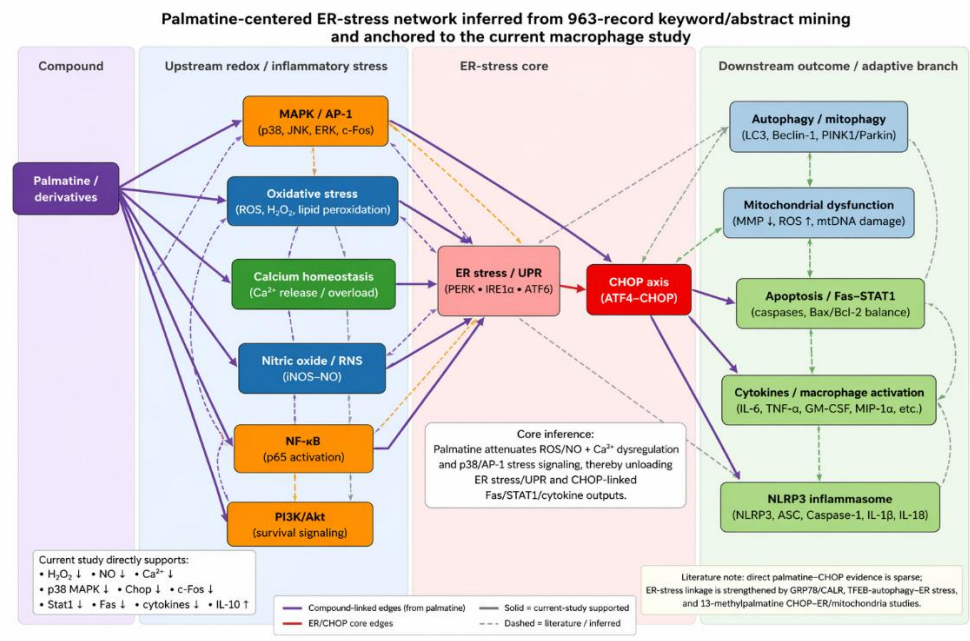

Figure 8. Network pharmacology-based schematic model of PA in ER stress-associated inflammatory responses. PA attenuates endotoxin-induced macrophage activation by targeting multiple interconnected signaling pathways. Upstream, PA suppresses excessive production of reactive oxygen species (ROS) and reactive nitrogen species (RNS), as well as cytosolic calcium release from the endoplasmic reticulum (ER). These effects contribute to the inhibition of ER stress and unfolded protein response signaling. PA also inhibits p38 MAPK activation and AP-1 (c-Fos) signaling, thereby reducing transcriptional activation of pro-inflammatory genes. At the ER stress level, PA downregulates CHOP expression, which is a key mediator of ER stress-induced apoptosis. Downstream, this results in decreased expression of STAT1 and Fas, leading to attenuation of apoptosis and inflammatory cell death. In parallel, PA reduces the production of pro-inflammatory cytokines (e.g., IL-6, TNF-α, GM-CSF) while enhancing anti-inflammatory IL-10 production.

These processes are tightly interconnected within the unfolded protein response and ER stress amplification pathways. In the present study, PA significantly reduced cytosolic calcium release, hydrogen peroxide production, and nitric oxide levels, while suppressing the transcription of Chop, Stat1, Fas, and c-Fos and inhibiting p38 MAPK activation in endotoxin-stimulated RAW 264.7 macrophages. These findings suggest that PA attenuates ER stress not only by directly downregulating CHOP expression but also by disrupting upstream feed-forward loops involving ROS accumulation, calcium dysregulation, and MAPK-mediated inflammatory signaling. This interpretation is supported by large-scale literature mining of 963 palmatine-related studies (Supplementary Table S2). In addition, from a network pharmacology perspective, PA can be interpreted as a multi-target regulator acting at the interface of redox balance, calcium signaling, and inflammatory pathways. By simultaneously modulating these interconnected nodes, PA may interrupt the propagation of ER stress toward CHOP-dependent apoptotic and inflammatory cascades. This integrative mechanism provides a plausible explanation for the broad anti-inflammatory and antioxidant effects of palmatine observed across diverse experimental models. Notably, the present study provides the first experimental evidence linking PA to the calcium–CHOP axis in macrophages, thereby bridging a critical gap between previously reported antioxidant and anti-inflammatory activities and ER stress-mediated cell death mechanisms, as summarized in Figure 8.

Despite these findings, the present study is limited to in vitro macrophage models. For example, the effects of PA on STAT activation and CAMKII transcription in activated macrophages were not investigated. Further studies addressing these aspects may provide a more detailed understanding

 doi:10.20944/preprints202605.0888.v1

of the mechanisms by which PA regulates ER stress. In addition, LPS triggers extracellular calcium influx through the action of ER-resident proteins (e.g., inositol trisphosphate receptors and stromal interaction molecules) and calcium channel proteins (e.g., transient receptor potential canonical channels and calcium release-activated calcium channel protein 1), and the effects of PA on such extracellular calcium influx were not evaluated in this study. It would also be meaningful to investigate the effects of PA on extracellular calcium influx and the activation of stromal interaction molecules in future studies. Taken together, these findings suggest that PA may serve as a promising multi-target modulator of ER stress-associated inflammatory responses, providing a potential therapeutic strategy for diseases involving dysregulated macrophage activation.

4. Materials and Methods

4.1. Materials

Dulbecco's modified Eagle medium, phosphate buffer saline, LPS, baicalein, and indomethacin were purchased from Millipore (Billerica, MA, USA). Although PA and palmatine are structurally similar, PA is more water-soluble than palmatine due to the presence of the positively charged quaternary ammonium ion, so PA was purchased from Millipore and used for experiments in this study. The experimental concentration (10 ~ 50 μM) of PA was set by referring to previous studies [48,49] using palmatine (10 ~ 100 mg/L). Baicalein was selected as a comparative substance because it had already been reported to alleviate the inflammation of macrophages induced by LPS [50].

4.2. Cell Viability

THP-1 human monocyte cell line (passage number 2) and RAW 264.7 mouse macrophage cell line (passage number 2) were obtained from the Korea Cell Line Bank (Seoul, Korea). Cells were incubated with PA for 24 h in 96-well plates ($1x10^4$ cells/well) to verify the toxicity of PA. After 24 h incubation with PA, cell viability was determined with a modified MTT assay [5–7]. The optical density (OD) was determined at 540 nm with a Model 680 microplate reader (Bio-Rad, Hercules, CA, USA).

4.3. NO Production, Cytosolic Calcium Level, and Hydrogen Peroxide Production

NO production was measured using Griess assay. After incubating cells ($1x10^4$ cells/well) with LPS and/or PA for 24 h, 100 μL of supernatant from each well was mixed with 100 μL Griess reagent in a 96-well plate. After 15 min of incubation at room temperature, the OD of each well was determined at 540 nm. Intracellular calcium level was measured with fluo-4 calcium assay. Cells in 96-well plates ($1x10^5$ cells/well) were incubated with LPS and/or PA for 24 h at 37 °C. Next, the medium was removed and cells were incubated with 100 μL of fluo-4 dye loading solution at 37 °C for 30 min. After incubation, the fluorescence intensity of each well was determined using a spectrofluorometer (Dynex, West Sussex, UK) with excitation and emission filters of 485 nm and 535 nm, respectively. The production of hydrogen peroxide in cells was measured with dihydrorhodamine (DHR) 123 Assay. Briefly, an aliquot of DHR was added to each well of a 96-well plate and pre-incubated at 37 °C for 30 min. The medium was then removed and cells were incubated with LPS and/or PA for 24 h or 48 h at 37 °C. After incubation, fluorescence intensities of wells were measured by a spectrofluorometer (Dynex) with an excitation filter at 485 nm and an emission filters 535 nm.

4.4. Cytokine Production

Cytokines produced by RAW 264.7 after 24 h of treatment were evaluated with MILLIPLEX MAP Mouse Cytokine/Chemokine Magnetic Bead Panel kits (Millipore). RAW 264.7 were seeded into 96-well plates ($1x10^4$ cells/well) and treated with LPS and/or PA. After 24 h of treatment, levels of the following cytokines in each well were analyzed. Briefly, the following procedures were

 doi:10.20944/preprints202605.0888.v1

performed. After pre-wetting a 96-well plate with Wash Buffer, the Wash Buffer was removed from each well using a Handheld Magnetic Separation Block (HMSB). Next, 25 µL of cell culture supernatant from each well was incubated with antibody-conjugated beads on a plate shaker for 2 h at room temperature. After incubation, well contents were gently removed with a HMSB and the 96-well plate was washed twice. Then 25 µL of Detection Antibodies was added to each well and incubated at room temperature with agitation on a plate shaker for 1 h. Subsequently, 25 µL Streptavidin–Phycoerythrin was added to each well containing Detection Antibodies and incubated for 30 min with agitation on a plate shaker at room temperature. After incubation, well contents were gently removed and washed twice with HMSB. Then 150 µL of Sheath Fluid was added to each well. Beads bound to each cytokine were analyzed with a Bio-Plex 200 instrument (Bio-Rad).

4.5. Transcripts of Inflammatory Genes

The mRNA levels of target genes such as *Chop*, *Stat1*, *Fas*, *c-Fos,* and *β-Actin* were quantified with real-time PCR using a Bio-Rad CFX 96 (Bio-Rad).

4.5.1. Isolation of RNA

RAW 264.7 mouse macrophages were incubated with LPS and/or PA for 18 h in 6-well plates (1x106 cells/well). After 18 h of incubation, total RNA for each well of cells was isolated using a NucleoSpin RNA kit (Macherey-Nagel, Duren, Germany). Briefly, 350 µL Lysis Buffer RA1 and 3.5 µL β-mercaptoethanol were added to cell pellet and vigorously vortexed to lyse cells. Lysate was cleared by filtration using a NucleoSpin® Filter. After 350 µL ethanol (70%) was added, cells were mixed by vortexing. Cell lysate was loaded into a NucleoSpin® RNA Column. After 350 µL Membrane Desalting Buffer was added, the column was centrifuged. Then 95 µL DNase reaction mixture was applied directly to the center of the silica membrane of the column, followed by incubation at room temperature for 15 min. Columns were washed with Wash Buffer RA2 and Wash Buffer RA3. After the silica membrane was dried, RNA was eluted with 60 µL RNase-free water and centrifuged.

4.5.2. Determination of RNA Concentration

RNA concentration was measured using an Experion RNA StdSens Analysis kit (Bio-Rad) with an Experion Automatic Electrophoresis System (Bio-Rad). First, electrodes were cleaned using a cleaning chip filled with 900 µL DEPC-treated water. After a gel-stain solution was then prepared, 9 µL of the solution was added into labeled wells, and the chip was primed. Samples and RNA ladder were loaded into the chip, which was then vortexed using an Experion vortex station for 1 min. Lastly, the chip was loaded into the electrophoresis platform and an RNA StdSens Analysis program was run.

4.5.3. cDNA Synthesis

cDNAs were synthesized using RNA samples and an iScript cDNA Synthesis kit (Bio-Rad). Briefly, 20 µL complete re-action mixes were prepared using 5x iScript Reaction Mix (4 µL), iScript Reverse Transcriptase (1 µL), Nuclease-free water (variable), and RNA template (variable, 1 µg total RNA). The reaction mix (20 µL) was incubated in a thermal cycler (C1000 Thermal Cycler, Bio-Rad) according to the manufacturer's protocol (priming at 25 °C for 5 min, reverse transcription at 46 °C for 20 min, and RT inactivation at 95 °C for 1 min).

4.5.4. Quantitative Real-Time PCR Analysis

Gene expression was measured using a quantitative polymerase chain reaction with an iQ SYBR Green Supermix (Bio-Rad) and a CFX96 Real-Time PCR Detection System (Bio-Rad). Briefly, a master mix was prepared for all reactions by adding iQ SYBR Green Supermix and forward/reverse primers for each target gene. This master mix was thoroughly mixed to ensure homogeneity. Then 7 µL was

 doi:10.20944/preprints202605.0888.v1

dispensed into each well of a qPCR plate. Next, 3 μL of cDNA was added to each well. Any air bubbles in the vessel bottom were removed. The PCR plate was loaded into the real-time PCR instrument. PCR was performed using the following cycling conditions: denaturation of DNA at 95 °C for 3 min, followed by 40 cycles of 95 °C for 10 sec and 55 °C for 30 sec. Relative mRNA expression levels were normalized against *β-actin* as an internal control and calculated with the $2^{-\Delta\Delta Ct}$ (Ct: cycle threshold) method. Table 2 lists the primers used in this study.

Table 2. Primers used in quantitative real-time PCR.

Name[1] (GenBank Accession Number)	Forward Primer (5′–3′)	Reverse Primer (5′–3′)
Chop (NM_007837)	CCACCACACCTGAAAGCAG	TCCTCATACCAGGCTTCCA
Fas (NM_009283.4)	CGCTGTTTTCCCTTGCTG	CCTTGAGTATGAACTCTTAACTGTGAG
Stat1 (NM_007987)	TGAGATGTCCCGGATAGTGG	CGCCAGAGAGAAATTCGTGT
c-Fos (NM_010234)	AGAGCGGGAATGGTGAAGA	TCTTCCTCTTCAGGAGATAGCTG
β-Actin (NM_007393.3)	CTAAGGCCAACCGTGAAAAG	ACCAGAGGCATACAGGGACA

[1]Primer names: C/EBP homologous protein (*Chop*), First apoptosis signal receptor (*Fas*), Signal Transducer and Activator of Transcription 1 (*Stat1*), *c-Fos*, and *β-Actin*.

4.6. Flow Cytometric Analysis for Levels of Phosphorylated p38 MAPK and Fas

RAW 264.7 was incubated with LPS and/or PA for 18 h in 6-well plates (3 x 10^5 cells/well). Phosphorylated p38 MAPK and Fas levels in RAW 264.7 were then evaluated via flow cytometry using an Attune NxT flow cytometer (Thermo Fisher Scientific, Waltham, MA, USA). Briefly, after 18 h of treatment, cells were stained with Fixable Viability Dye eFluor 520 (eBioscience 65-0867-18), phospho-p38 MAPK (T180/Y182) Monoclonal Antibody (eBioscience 17-9078-42), CD95 (APO-1/Fas) Monoclonal Antibody (eBioscience 12-0951-83), mouse IgG1 kappa isotype control (eBioscience 12-4714-81), and mouse IgG2b kappa isotype control (eBioscience 12-4732-81) according to the manufacturer's protocol. Fixable Viability Dye eFluor 520 was used to irreversibly label dead cells prior to cryopreservation, fixation, and/or permeabilization procedures. Cells were fixed with a Fix Buffer (Thermo Fisher Scientific), permeabilized with a Perm Buffer (Thermo Fisher Scientific), and stained with fluorescent-labeled antibodies. Stained cells were analyzed with an Attune NxT flow cytometer. A serial gating strategy used forward scatter versus side scatter plots, forward scatter versus viability stain plots, and target antibody expression plots. Unstained cells were used as negative controls for gating. Data were obtained from the mean fluorescent intensities of samples. Details regarding startup, proper calibration, and operation of the Attune NxT flow cytometer can be found in the Attune User Guide (https://assets.thermofisher.com/TFS-Assets/LSG/manuals/100024235_AttuneNxT_HW_UG.pdf).

4.7. Statistical Analyses

Data are representatives of at least three independent experiments. Values are expressed as means ± standard deviation (SD). All data were subjected to a one-way analysis of variance (ANOVA) followed by Tukey's multiple comparison test using GraphPad Prism (version 4; GraphPad Software, San Diego, CA, USA).

 doi:10.20944/preprints202605.0888.v1

4.8. Network Pharmacology Analysis

To explore the potential mechanisms of PA beyond the experimental findings, a network pharmacology-informed analysis was conducted based on literature mining. A total of 963 palmatine-related articles were collected and curated from published literature sources, and the full list is provided in Supplementary Table S2. Keywords and abstracts were analyzed to identify frequently co-occurring biological processes, signaling pathways, and molecular targets associated with palmatine. Target-related terms were manually standardized and categorized into functional groups, including oxidative stress, inflammatory signaling, apoptosis, autophagy, and endoplasmic reticulum (ER) stress-related pathways. Based on these data, a compound–target–pathway interaction network was constructed. Key nodes were selected according to their frequency of occurrence and biological relevance to macrophage activation and ER stress. The network was visualized using Cytoscape software (version 3.10.4), and node–edge relationships were defined to represent interactions among palmatine, molecular targets, and signaling pathways. In addition, a mock enrichment analysis was performed to identify representative Gene Ontology terms and Kyoto Encyclopedia of Genes and Genomes pathways associated with the extracted targets. This analysis was conducted as a literature-informed approximation to support mechanistic interpretation rather than a database-driven enrichment test. The dataset was used for qualitative network inference rather than quantitative meta-analysis. In the preparation of this section, a generative artificial intelligence tool (ChatGPT, OpenAI) was used to assist in organizing literature-derived information and drafting descriptive text related to network pharmacology. The identification of key pathways, interpretation of biological mechanisms, and all scientific conclusions were independently performed and critically evaluated by the authors.

5. Conclusions

PA exerts anti-inflammatory effects on endotoxin-stimulated RAW 264.7 cells via the calcium-CHOP pathway, consequently reducing endotoxin-induced production of pro-inflammatory mediators (e.g., NO and cytokines) and alleviating ER stress-related pyroptotic cascade, highlighting its potential as a multi-target therapeutic agent for ER stress-associated inflammatory diseases.

Supplementary Materials: The following supporting information can be downloaded at the website of this paper posted on Preprints.org: Method S1: Detailed experimental procedures; Supplementary Table S2: Complete list of 963 palmatine-related articles used for literature mining and network pharmacology-informed analysis.

Author Contributions: Conceptualization, W.P.; methodology, W.P.; validation, W.P.; investigation, Y.-J.K. and W.P.; resources, Y.-J.K. and W.P.; writing—original draft preparation, W.P.; writing—review and editing, S.S.N. and W.P.; visualization, W.P.; supervision, S.S.N. and W.P.; funding acquisition, W.P. All authors have read and agreed to the published version of the manuscript.

Funding: This work was supported by the National Research Foundation of Korea (NRF) grant funded by the Korea government (MSIT) (RS-2025-24523909).

Institutional Review Board Statement: Not applicable.

Informed Consent Statement: Not applicable.

Data Availability Statement: The data presented in this study are available on request from the corresponding author.

Acknowledgments: The authors thank Ji-Young Lee and Hyun-Joo Kim (College of Korean Medicine, Gachon University) for their technical assistance.

Conflicts of Interest: The authors have no conflicts of interest relevant to this study to disclose. The funders had no role in the design of this study, data collection, data analyses, data interpretation, writing of the manuscript, or the decision to publish the results.

 doi:10.20944/preprints202605.0888.v1

References

1. Tanwar, J.; Das, S.; Fatima, Z.; Hameed, S. Multidrug Resistance: An Emerging Crisis. Interdiscip. Perspect. Infect. Dis. **2014**, *2014*, 541340.
2. Saha, M.; Sarkar, A. Review on Multiple Facets of Drug Resistance: A Rising Challenge in the 21st Century. J. Xenobiot **2021**, *11*, 197-214.
3. Maczka, W.; Duda-Madej, A.; Grabarczyk, M.; Winska, K. Natural Compounds in the Battle Against Microorganisms-Linalool. Molecules **2022**, *27*, 6928.
4. Feitosa, B.F.; de Alcantara, C.M.; de Lima, Amanda Beatriz Sales; Silva, A.S.; Araujo, A.D.S.; Cavalcanti, M.T.; Mori, E.; Araujo, I.M.; de Farias, Pablo Antonio Maia; Wilairatana, P. et al. Bioactive Natural Products for Chemical Control of Microorganisms: Scientific Prospecting (2001-2021) and Systematic Review. Molecules **2022**, *27*, 5917.
5. Kim, D.H.; Lee, J.Y.; Kim, Y.J.; Kim, H.J.; Park, W. Rubi Fructus Water Extract Alleviates LPS-Stimulated Macrophage Activation Via an ER Stress-Induced Calcium/CHOP Signaling Pathway. Nutrients **2020**, *12*, 3577.
6. Kim, Y.J.; Lee, J.Y.; Kim, H.J.; Kim, D.H.; Lee, T.H.; Kang, M.S.; Park, W. Anti-Inflammatory Effects of Angelica Sinensis (Oliv.) Diels Water Extract on RAW 264.7 Induced with Lipopolysaccharide. Nutrients **2018**, *10*, 647.
7. An, H.; Lee, J.; Park, W. Baicalin Modulates Inflammatory Response of Macrophages Activated by LPS Via Calcium-CHOP Pathway. Cells **2022**, *11*, 3076.
8. Rietschel, E.T.; Kirikae, T.; Schade, F.U.; Mamat, U.; Schmidt, G.; Loppnow, H.; Ulmer, A.J.; Zahringer, U.; Seydel, U.; Di Padova, F. Bacterial Endotoxin: Molecular Relationships of Structure to Activity and Function. FASEB J. **1994**, *8*, 217-225.
9. Moran, A.P.; Prendergast, M.M.; Appelmelk, B.J. Molecular Mimicry of Host Structures by Bacterial Lipopolysaccharides and its Contribution to Disease. FEMS Immunol. Med. Microbiol. **1996**, *16*, 105-115.
10. Tabas, I. Macrophage Apoptosis in Atherosclerosis: Consequences on Plaque Progression and the Role of Endoplasmic Reticulum Stress. Antioxid. Redox Signal. **2009**, *11*, 2333-2339.
11. Tabas, I. The Role of Endoplasmic Reticulum Stress in the Progression of Atherosclerosis. Circ. Res. **2010**, *107*, 839-850.
12. Klymenko, O.; Huehn, M.; Wilhelm, J.; Wasnick, R.; Shalashova, I.; Ruppert, C.; Henneke, I.; Hezel, S.; Guenther, K.; Mahavadi, P.; et al. Regulation and Role of the ER Stress Transcription Factor CHOP in Alveolar Epithelial Type-II Cells. *J. Mol. Med.* **2019**, *97*, 973–990.
13. Chen, L.; Song, C.; Zhang, Y.; Li, Y.; Zhao, Y.; Lin, F.; Han, D.; Dai, M.; Li, W.; Pan, P. Quercetin Protects Against LPS-Induced Lung Injury in Mice Via SIRT1-Mediated Suppression of PKM2 Nuclear Accumulation. Eur. J. Pharmacol. **2022**, *936*, 175352.
14. Feng, M.; Wei, S.; Zhang, S.; Yang, Y. Anti-Inflammation and Anti-Pyroptosis Activities of Mangiferin Via Suppressing NF-kappaB/NLRP3/GSDMD Signaling Cascades. Int. J. Mol. Sci. **2022**, *23*, 10124.
15. Li, G.; Mongillo, M.; Chin, K.; Harding, H.; Ron, D.; Marks, A.R.; Tabas, I. Role of ERO1-Alpha-Mediated Stimulation of Inositol 1,4,5-Triphosphate Receptor Activity in Endoplasmic Reticulum Stress-Induced Apoptosis. J. Cell Biol. **2009**, *186*, 783-792.
16. Tabas, I.; Seimon, T.; Timmins, J.; Li, G.; Lim, W. Macrophage Apoptosis in Advanced Atherosclerosis. Ann. N. Y. Acad. Sci. **2009**, *1173 Suppl 1*, E40-5.
17. Timmins, J.M.; Ozcan, L.; Seimon, T.A.; Li, G.; Malagelada, C.; Backs, J.; Backs, T.; Bassel-Duby, R.; Olson, E.N.; Anderson, M.E. et al. Calcium/calmodulin-Dependent Protein Kinase II Links ER Stress with Fas and Mitochondrial Apoptosis Pathways. J. Clin. Invest. **2009**, *119*, 2925-2941.
18. Li, D.; Ren, W.; Jiang, Z.; Zhu, L. Regulation of the NLRP3 Inflammasome and Macrophage Pyroptosis by the p38 MAPK Signaling Pathway in a Mouse Model of Acute Lung Injury. Mol. Med. Rep. **2018**, *18*, 4399-4409.
19. Wang, X.Z.; Ron, D. Stress-Induced Phosphorylation and Activation of the Transcription Factor CHOP (GADD153) by p38 MAP Kinase. Science **1996**, *272*, 1347-1349.

 doi:10.20944/preprints202605.0888.v1

20. Endo, M.; Mori, M.; Akira, S.; Gotoh, T. C/EBP Homologous Protein (CHOP) is Crucial for the Induction of Caspase-11 and the Pathogenesis of Lipopolysaccharide-Induced Inflammation. J. Immunol. **2006**, *176*, 6245-6253.
21. Krupkova, O.; Sadowska, A.; Kameda, T.; Hitzl, W.; Hausmann, O.N.; Klasen, J.; Wuertz-Kozak, K. P38 MAPK Facilitates Crosstalk between Endoplasmic Reticulum Stress and IL-6 Release in the Intervertebral Disc. Front. Immunol. **2018**, *9*, 1706.
22. Vodovotz, Y.; Kim, P.K.M.; Bagci, E.Z.; Ermentrout, G.B.; Chow, C.C.; Bahar, I.; Billiar, T.R. Inflammatory Modulation of Hepatocyte Apoptosis by Nitric Oxide: In Vivo, in Vitro, and in Silico Studies. Curr. Mol. Med. **2004**, *4*, 753-762.
23. Rudkowski, J.C.; Barreiro, E.; Harfouche, R.; Goldberg, P.; Kishta, O.; D'Orleans-Juste, P.; Labonte, J.; Lesur, O.; Hussain, S.N.A. Roles of iNOS and nNOS in Sepsis-Induced Pulmonary Apoptosis. Am. J. Physiol. Lung Cell. Mol. Physiol. **2004**, *286*, L793-800.
24. Bove, P.F.; van der Vliet, A. Nitric Oxide and Reactive Nitrogen Species in Airway Epithelial Signaling and Inflammation. Free Radic. Biol. Med. **2006**, *41*, 515-527.
25. Mori, M. Regulation of Nitric Oxide Synthesis and Apoptosis by Arginase and Arginine Recycling. J. Nutr. **2007**, *137*, 1616S-1620S.
26. Nakayama, Y.; Endo, M.; Tsukano, H.; Mori, M.; Oike, Y.; Gotoh, T. Molecular Mechanisms of the LPS-Induced Non-Apoptotic ER Stress-CHOP Pathway. J. Biochem. **2010**, *147*, 471-483.
27. Gotoh, T.; Mori, M. Nitric Oxide and Endoplasmic Reticulum Stress. Arterioscler. Thromb. Vasc. Biol. **2006**, *26*, 1439-1446.
28. Gotoh, T.; Oyadomari, S.; Mori, K.; Mori, M. Nitric Oxide-Induced Apoptosis in RAW 264.7 Macrophages is Mediated by Endoplasmic Reticulum Stress Pathway Involving ATF6 and CHOP. J. Biol. Chem. **2002**, *277*, 12343-12350.
29. Zeeshan, H.M.A.; Lee, G.H.; Kim, H.; Chae, H. Endoplasmic Reticulum Stress and Associated ROS. Int. J. Mol. Sci. **2016**, *17*, 327.
30. Haynes, C.M.; Titus, E.A.; Cooper, A.A. Degradation of Misfolded Proteins Prevents ER-Derived Oxidative Stress and Cell Death. Mol. Cell **2004**, *15*, 767-776.
31. Malhotra, J.D.; Miao, H.; Zhang, K.; Wolfson, A.; Pennathur, S.; Pipe, S.W.; Kaufman, R.J. Antioxidants Reduce Endoplasmic Reticulum Stress and Improve Protein Secretion. Proc. Natl. Acad. Sci. U. S. A. **2008**, *105*, 18525-18530.
32. Seimon, T.A.; Obstfeld, A.; Moore, K.J.; Golenbock, D.T.; Tabas, I. Combinatorial Pattern Recognition Receptor Signaling Alters the Balance of Life and Death in Macrophages. Proc. Natl. Acad. Sci. U. S. A. **2006**, *103*, 19794-19799.
33. Cookson, B.T.; Brennan, M.A. Pro-Inflammatory Programmed Cell Death. Trends Microbiol. **2001**, *9*, 113-114.
34. Jorgensen, I.; Miao, E.A. Pyroptotic Cell Death Defends Against Intracellular Pathogens. Immunol. Rev. **2015**, *265*, 130-142.
35. Gong, W.; Shi, Y.; Ren, J. Research Progresses of Molecular Mechanism of Pyroptosis and its Related Diseases. Immunobiology **2020**, *225*, 151884.
36. Slomiany, B.L.; Slomiany, A. Involvement of p38 MAPK-Dependent Activator Protein (AP-1) Activation in Modulation of Gastric Mucosal Inflammatory Responses to Helicobacter Pylori by Ghrelin. Inflammopharmacology **2013**, *21*, 67-78.
37. Mandrekar, P.; Szabo, G. Signalling Pathways in Alcohol-Induced Liver Inflammation. J. Hepatol. **2009**, *50*, 1258-1266.
38. Mechta-Grigoriou, F.; Gerald, D.; Yaniv, M. The Mammalian Jun Proteins: Redundancy and Specificity. Oncogene **2001**, *20*, 2378-2389.
39. Klymenko, O.; Huehn, M.; Wilhelm, J.; Wasnick, R.; Shalashova, I.; Ruppert, C.; Henneke, I.; Hezel, S.; Guenther, K.; Mahavadi, P. et al. Regulation and Role of the ER Stress Transcription Factor CHOP in Alveolar Epithelial Type-II Cells. J. Mol. Med. (Berl) **2019**, *97*, 973-990.
40. Kim, H.; Kim, Y.; Park, W. Berberine Modulates Hyper-Inflammation in Mouse Macrophages Stimulated with Polyinosinic-Polycytidylic Acid Via Calcium-CHOP/STAT Pathway. Sci. Rep. **2021**, *11*, 11298.

 doi:10.20944/preprints202605.0888.v1

41. Long, J.; Song, J.; Zhong, L.; Liao, Y.; Liu, L.; Li, X. Palmatine: A Review of its Pharmacology, Toxicity and Pharmacokinetics. Biochimie **2019**, *162*, 176-184.
42. Tarabasz, D.; Kukula-Koch, W. Palmatine: A Review of Pharmacological Properties and Pharmacokinetics. Phytother. Res. **2020**, *34*, 33-50.
43. Ekeuku, S.O.; Pang, K.; Chin, K. Palmatine as an Agent Against Metabolic Syndrome and its Related Complications: A Review. Drug Des. Devel. Ther. **2020**, *14*, 4963-4974.
44. Ativui, S.; Danquah, C.A.; Ossei, P.P.S.; Ofori, M. Palmatine Attenuates Metastatic Lung Colonization of Triple Negative Breast Cancer Cells. Front. Pharmacol. **2022**, *13*, 853230.
45. Wang, L.; Wang, X.; Zhang, S.; Zhu, X.; Liu, Y.; Song, Z.; Du, W.; Ji, J.; Cui, C.; He, X. et al. Gastroprotective Effect of Palmatine Against Acetic Acid-Induced Gastric Ulcers in Rats. J. Nat. Med. **2017**, *71*, 257-264.
46. Zhang, X.; Yuan, Z.; Qu, C.; Yu, X.; Huang, T.; Chen, P.V.; Su, Z.; Dou, Y.; Wu, J.; Zeng, H. et al. Palmatine Ameliorated Murine Colitis by Suppressing Tryptophan Metabolism and Regulating Gut Microbiota. Pharmacol. Res. **2018**, *137*, 34-46.
47. Ma, W.; Li, H.; Dong, C.; He, X.; Guo, C.; Zhang, C.; Yu, C.; Wang, C.; Yuan, C. Palmatine from Mahonia Bealei Attenuates Gut Tumorigenesis in ApcMin/+ Mice Via Inhibition of Inflammatory Cytokines. Mol. Med. Rep. **2016**, *14*, 491-498.
48. Zhou, X.; Lin, X.; Xiong, Y.; Jiang, L.; Li, W.; Li, J.; Wu, L. Chondroprotective effects of palmatine on osteoarthritis in vivo and in vitro: A possible mechanism of inhibiting the Wnt/β-catenin and Hedgehog signaling pathways. Int. Immunopharmacol. **2016**, *34*, 129-138.
49. Yang, Q.C.; Wu, W.H.; Han, F.M.; Chen, Y. Identification of in-vivo and in-vitro metabolites of palmatine by liquid chromatography-tandem mass spectrometry. J. Pharm. Pharmacol. **2009**, *61*, 647-652.
50. Fan, G.W.; Zhang, Y.; Jiang, X.; Zhu, Y; Wang, B.; Su, L.; Cao, W.; Zhang, H.; Gao, X. Anti-inflammatory activity of baicalein in LPS-stimulated RAW264.7 macrophages via estrogen receptor and NF-κB-dependent pathways. Inflammation. **2013**, *36*, 1584-91.
51. Wang, J.; Wang, L.; Lou, G.; Zeng, H.; Hu, J.; Huang, Q.; Peng, W.; Yang, X. Coptidis Rhizoma: A Comprehensive Review of its Traditional Uses, Botany, Phytochemistry, Pharmacology and Toxicology. Pharm. Biol. **2019**, *57*, 193-225.
52. Sun, Y.; Lenon, G.B.; Yang, A.W.H. Phellodendri Cortex: A Phytochemical, Pharmacological, and Pharmacokinetic Review. Evid Based. Complement. Alternat Med. **2019**, *2019*, 7621929.